Optical limiting properties and z-scan measurements of carbon disulfide at 2.05 μm wavelength

LARS GRØNMARK HOLMEN[1] AND MAGNUS W. HAAKESTAD[1,*]

[1] Norwegian Defence Research Establishment (FFI), P O Box 25, NO-2027 Kjeller, Norway
[*] Corresponding author: Magnus-W.Haakestad@ffi.no

Compiled June 17, 2016

Nonlinear and optical limiting properties of carbon disulfide (CS_2) are characterized at 2.05 μm wavelength using a Q-switched Ho:YLF laser with high pulse energy. The nonlinear refractive index of CS_2 is measured using the z-scan technique, giving a value of (1.9±0.5)·10^{-18} m^2/W, i.e. (7.2±1.9)·10^{-12} esu, for the 25 ns pulses from the Ho:YLF laser. Self-focusing and dielectric breakdown in CS_2 limited the output energy to 0.6 mJ in the optical limiting experiments for input energies of up to 150 mJ.

OCIS codes: *(160.4330) Nonlinear optical materials; (190.4360) Nonlinear optics, devices; (190.4400) Nonlinear optics, materials; (230.4320) Nonlinear optical devices; (260.5950) Self-focusing.*

http://dx.doi.org/10.1364/ao.XX.XXXXXX

1. INTRODUCTION

When an electro-optic sensor focuses the incident radiation onto a detector the intensity is typically increased by a factor 10^6 to 10^7. This means that the detector elements can be easily damaged if the sensor is illuminated by a laser. The damage threshold of semiconductor materials is typically of the order of 1 J/cm^2 for pulse durations of a few tens of nanoseconds [1]. If the sensor is focusing the radiation down to a diameter of 10 μm, damage will occur if the pulse energy exceeds about 1 μJ, which corresponds to 50 nJ/cm^2 incident on a 50 mm aperture. A laser can readily deliver such a fluence from a long range.

One way of protecting a sensor against damage from laser pulses is to use an optical filter that blocks the most common laser wavelengths. This is however not a safe method, due to the development of laser sources with new or tunable wavelengths. Another solution is to use an optical limiter, which is a passive device that blocks radiation with high intensity and transmits radiation with low intensity [2, 3]. This is achieved by focusing the radiation down to a small spot in the optical limiter material, which has a nonlinear optical response. Relevant nonlinear mechanisms include self-focusing, dielectric breakdown, and free-carrier absorption [4, 5]. For defense applications, there are several sensors operating in the wavelength ranges 1.5–2.5 μm, 3–5 μm, and 8–12 μm, where the atmosphere has high transmission. It is thus of interest to characterize properties of optical limiters in these wavelength regions. An optical limiter material should not be damaged by laser pulses with high energy. This makes liquids attractive candidates as optical limiter materials, because liquids are not locally damaged, in contrast to solids. Carbon disulfide (CS_2) is a liquid with an especially high nonlinear refractive index [6], and it has previously been used as an optical limiting material in the visible range, at 0.7–1.1 μm wavelength, and at 10.6 μm [3, 7, 8].

In this paper we characterize the nonlinear and optical limiting properties of CS_2 at 2.05 μm wavelength using pulses with up to 150 mJ energy from a Q-switched Ho:YLF laser [9]. The nonlinear refractive index of CS_2 is measured at 2.05 μm using the z-scan technique [10], and the obtained value of (1.9±0.5)·10^{-18} m^2/W, i.e. (7.2±1.9)·10^{-12} esu, for the nonlinear coefficient is in reasonable agreement with previous experiments using similar pulse duration at shorter wavelengths [11, 12]. We show that the average nonlinear phase shift is a factor $(2 - N^{-1})$ larger for a multiple-longitudinal mode (MLM) pulse, compared to a single-longitudinal mode (SLM) pulse, where N is the number of longitudinal modes. This result is similar to the case of second-harmonic generation of a MLM laser [13, 14].

This paper gives a more detailed description of the CS_2 experiments presented at a recent conference [15]. To our knowledge, these are the first z-scan and optical limiting experiments performed at 2 μm with CS_2. In Section 2, we summarize the optical properties of CS_2 relevant for optical limiting. The experimental setup for z-scan measurements and optical limiting experiments are described in Section 3, while the results are shown in Section 4. A derivation of the nonlinear phase-shift for MLM pulses is presented in Appendix A.

2. OPTICAL PROPERTIES OF CS_2

The transmission through a 20 mm thick CS_2 cell was measured in the wavelength range 2–5.5 μm using an FTIR spectrometer and the results are shown in Fig. 1. The measured transmission

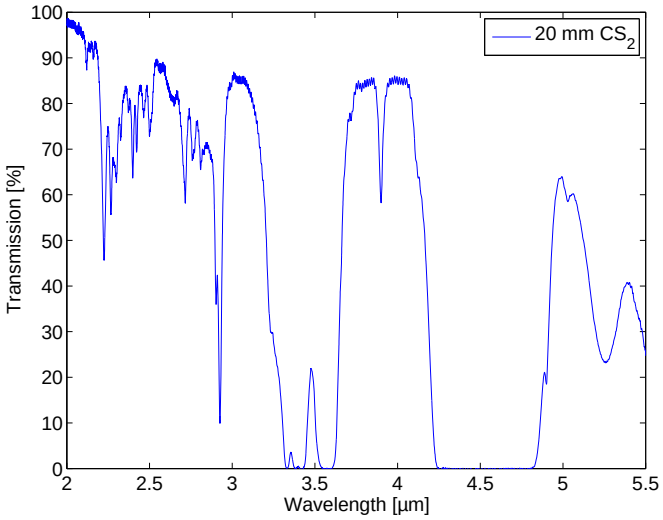

Fig. 1. Measured transmission through 20 mm CS_2 corrected for reflection losses of the cell windows.

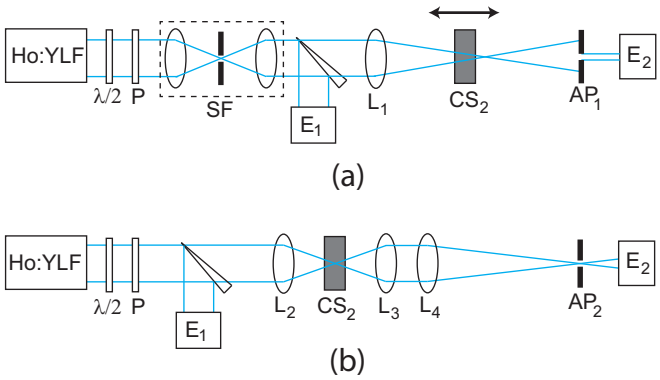

Fig. 2. Schematic of the experimental setup. (a) z-scan measurements and (b) optical limiting experiments. $\lambda/2$: half-wave plate, P: polarizer, SF: spatial filter, E_1 reference energy meter, L_1-L_4: lenses with focal lengths, 20 cm, 5 cm, 5 cm, and 100 cm, respectively, CS_2: CS_2 cell with uncoated sapphire windows, AP_1: adjustable aperture, AP_2: aperture with 1.4 mm diameter, E_2 energy meter.

at 2.05 μm is 96.9%, corresponding to an absorption coefficient of α_0=1.6/m at this wavelength. This is sufficiently low for limiting applications at 2.05 μm, but we observe from the figure that CS_2 is not suitable as an optical limiter material in the entire 2–5.5 μm region due to the existence of a number of strong absorption bands. The measured transmission in Fig. 1 agrees reasonably well with previous results for CS_2 [16]. At 2.05 μm wavelength, the refractive index of CS_2 is $n_0 = 1.59$ [17]. Ganeev et al. and Reichert et al. present measurements of the nonlinear coefficient of CS_2 for various pulse durations [11, 12]. They find that it increases from $\gamma = 3 \cdot 10^{-19}$ m^2/W ($1.1 \cdot 10^{-12}$ esu) for a pulse duration of 110 fs to $4 \cdot 10^{-18}$ m^2/W ($1.5 \cdot 10^{-11}$ esu) at a pulse duration of 75 ns. These values refer to measurements carried out at visible and near-infrared wavelengths. Several other measured values of the nonlinear properties of CS_2 are given in Refs. [18–21]. However, the nonlinear properties of CS_2 near 2 μm wavelength have to our knowledge not been reported before. The dependence of the nonlinear coefficient on the pulse duration is due to the contribution of different mechanisms on different time scales. For CS_2 these contributions come mainly from bound electrons (femtosecond time scale), molecular reorientation (picosecond time scale), electrostriction (nanosecond time scale), and thermal effects ($>$ 10 ns time scale) [2, 12, 22].

3. EXPERIMENTAL SETUP

The experimental setups for the z-scan measurements and optical limiting experiments are shown in Fig. 2(a) and (b), respectively. A Q-switched Ho:YLF laser was used in both experiments. This laser provides up to 550 mJ pulse energy at $\lambda = 2.05$ μm wavelength, with a beam quality $M^2 = 1.5$ (the beam quality indicates how much a beam diverges as it propagates, compared to a Gaussian beam) [9]. It has a spectral bandwidth (FWHM) of $\Delta\nu_L$ =29 GHz and operates on multiple longitudinal modes. The FWHM pulse duration was 25 ns. A half-wave plate and a polarizer was used to vary the input energy onto the CS_2 cell. A pulse energy of up to 150 mJ was used in the experiments, limited by the damage threshold of the 5 mm thick uncoated sapphire windows in the CS_2 cell, which is about 200 J/cm^2 [23].

A. z-scan measurements

A spatial filter was used in the z-scan measurements to obtain a near Gaussian beam profile with a FWe^{-2}M beam diameter of $D = 5.2$ mm. The spatial filter consisted of a pinhole with diameter 50 μm and two lenses, both with focal length 10 cm. The focal length of L_1 was $f_1 = 20$ cm. This gives an estimated beam diameter in the focus position of $d = 4\lambda f_1/(D\pi)$ =100 μm for a Gaussian beam, which corresponds to a Rayleigh length of 6.1 mm in the CS_2 cell. The measured beam diameter of 110 μm in the focus position agrees reasonably well with the calculated value for a Gaussian beam. The length of the CS_2 cell was 5 mm in the z-scan measurements. This is sufficiently short to make use of the thin sample approximation, which applies when the length of the sample cell is less than the Rayleigh length in the sample medium [24]. During the z-scan measurements the laser was operated with a repetition rate of 10 Hz and a pulse energy of 1.0 mJ incident onto the CS_2 liquid. The measured linear absorption of 3.1% in a 20 mm long sample cell corresponds to an absorption of 0.8% for the 5 mm thick sample cell in the z-scan measurements, which is negligible. The distance between the adjustable aperture AP_1 and the CS_2 cell was 25 cm in these measurements.

B. Optical limiting experiments

In the optical limiting experiments, the spatial filter (SF) was removed, as shown in Fig. 2(b), to maximize the pulse energy into the CS_2 cell. The limiter itself consists of the lenses L_2 and L_3, together with a 20 mm long CS_2 cell. The lens L_4, with focal length 1 m, and the aperture AP_2 can be considered as a sensor unit, and the task of the limiter is to reduce the maximum fluence at the sensor plane, here represented by AP_2. L_2 and L_3 had both a focal length of 50 mm, which gives an effective f-number of about 10 for the optical limiter. This gave a measured beam diameter of 32 μm in the focus position in the CS_2 cell. The focus position was 5 mm before the back window of the cell, because damage on the front window was observed when the focus position was in the middle of the cell. The focus is reimaged with magnification 20 onto the aperture AP_2, which had a diameter of 1.4 mm. This was the smallest aperture that gave good ($>$ 99%) transmission at low pulse energies. The

energy transmitted through AP_2 is denoted the focusable energy [2], which is one important characteristic of an optical limiter. In addition to measuring the focusable energy, the beam profile in the position of AP_2 was imaged by a pyroelectric camera, to obtain more detailed information about the fluence distribution of the beam. The repetition rate of the Ho:YLF laser was 1 Hz during the optical limiting experiments.

4. RESULTS

A. z-scan

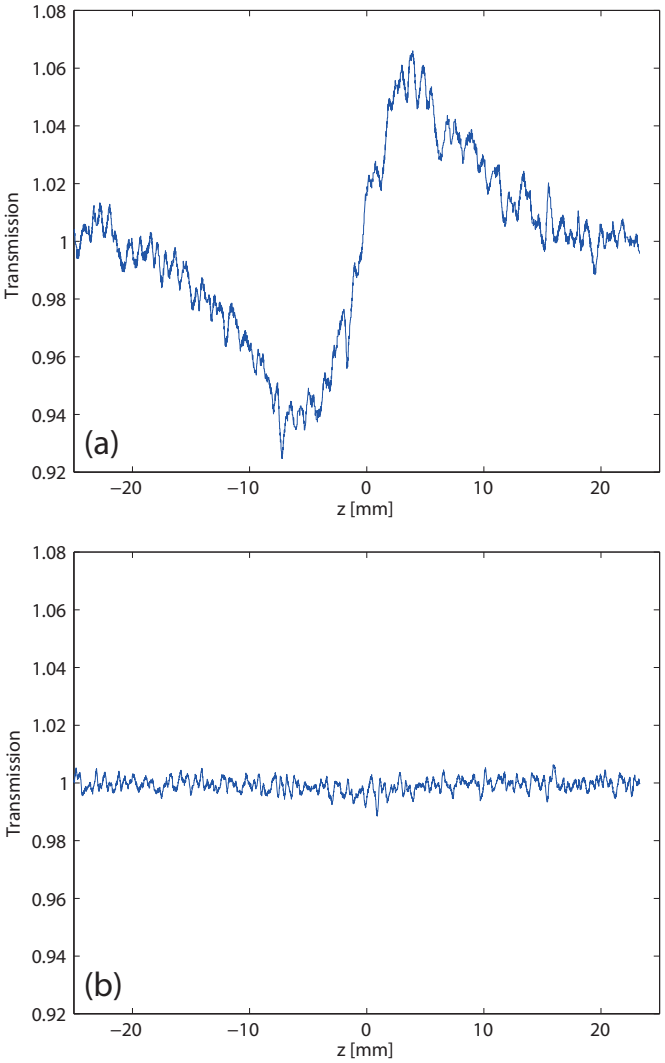

Fig. 3. Measured transmission for a z-scan with (a) small aperture and (b) open aperture.

A z-scan measurement where the diameter of AP_1 was adjusted to give a transmission $S = 0.3$ was carried out. Raw data from this measurement is shown in Fig. 3(a). In absence of nonlinear absorption, the change ΔT_{pv} in transmission between the peak and the valley is given by [24]

$$\Delta T_{pv} = 0.41\,(1-S)^{0.27}\,|\langle \Delta\Phi_0(t)\rangle|, \tag{1}$$

where

$$\langle \Delta\Phi_0(t)\rangle = \frac{\int_{-\infty}^{\infty} \Delta\Phi_0(t) I_0(t)\mathrm{d}t}{\int_{-\infty}^{\infty} I_0(t)\mathrm{d}t} \tag{2}$$

and

$$\Delta\Phi_0(t) = \frac{2\pi}{\lambda}\gamma I_0(t) L_{\text{eff}}. \tag{3}$$

$I_0(t)$ is the peak intensity in the focus position and $L_{\text{eff}} = [1-\exp(-\alpha_0 L)]/\alpha_0$ is the effective sample length, which to a good approximation is equal to the physical sample length L in this case. If the pulse has a Gaussian profile, we have $\langle \Delta\Phi_0(t)\rangle = \Delta\Phi_0/\sqrt{2}$, where $\Delta\Phi_0$ is the maximum nonlinear phase shift. To obtain a near Gaussian pulse profile, the laser needs to oscillate on a single longitudinal mode. The laser used in these experiments oscillated on $N \approx \Delta\nu_L/\Delta\nu_{\text{fsr}} \approx 100$ longitudinal modes, where $\Delta\nu_{\text{fsr}} = 0.2$ GHz is the free spectral range of the laser cavity. This leads to intensity fluctuations with duration $1/\Delta\nu_L \approx 30$ ps. We show in Appendix A that $\langle \Delta\Phi_0(t)\rangle$ increases by a factor $\left(2-N^{-1}\right) \approx 2$ for a MLM pulse, compared to a SLM pulse, assuming that the coherence time of the laser is long compared to the response time of CS_2. The fact that $\langle \Delta\Phi_0(t)\rangle$ increases for MLM pulses has previously been demonstrated experimentally [25].

From Fig. 3, we find that $\Delta T_{pv} = 0.12$. This gives an average nonlinear phase shift $\langle \Delta\Phi_0(t)\rangle = 0.32$ according to Eq. (1). For a pulse energy of 1.0 mJ, a pulse duration of 25 ns, and a beam diameter of 110 μm, we obtain a peak intensity $I_0 = 7.9\ \text{TW/m}^2$ for a Gaussian pulse. By taking into account that the pulse is MLM, we obtain $\gamma = (1.9 \pm 0.5)\cdot 10^{-18}\ \text{m}^2/\text{W}$, i.e. $(7.2\pm1.9)\cdot 10^{-12}$ esu, where the uncertainty is estimated from the uncertainty in the experimental parameters. For comparison, Ganeev et al. have measured a nonlinear coefficient of $\gamma = 3\cdot 10^{-18}\ \text{m}^2/\text{W}$ ($1.1\cdot 10^{-11}$ esu) for 20 ns long pulses at 532 nm wavelength from a frequency-doubled Nd:YAG laser [11], but it was not stated if the laser was SLM or MLM.

The transmission coefficient for a Gaussian pulse in an open-aperture z-scan measurement is given by

$$T = 1 - \frac{1}{2\sqrt{2}}\frac{\beta I_0 L_{\text{eff}}}{1+\frac{z^2}{z_0^2}}, \tag{4}$$

where β is the nonlinear absorption coefficient and z_o is the Rayleigh range of the beam in air [24]. Similar to the case with $\langle \Delta\Phi_0(t)\rangle$, it can be shown that $T-1$ increases by a factor $\left(2-N^{-1}\right) \approx 2$ for a MLM pulse, compared to a SLM pulse. During z-scan measurements with open aperture, we did not observe any significant change of the transmission, as shown in Fig. 3(b). From the figure, we conclude that $T > 0.995$, giving $\beta I_0 L < 0.007$ and $\beta < 2\cdot 10^{-13}\ \text{m/W}$, which would not have any significant influence on the z-scan measurements with small aperture.

B. Optical limiting

B.1. Observation of dielectric breakdown

When the pulse energy into the CS_2 cell exceeded about 0.8 mJ in the optical limiting experiments (Fig. 2(b)), a visible spark was observed in the focus position, due to plasma generated by dielectric breakdown. Well above the threshold for dielectric breakdown, an elongation of the spark was observed, in agreement with previous observations [3]. Images of the spark at different input energies are shown in Fig. 4. According to the moving-focus model [5], the focus position of a nanosecond pulse experiencing self-focusing will extend over an interval from the original focus position and towards the input window, due to the time-varying pulse power. We observed that the elongation of the breakdown region extended towards the input

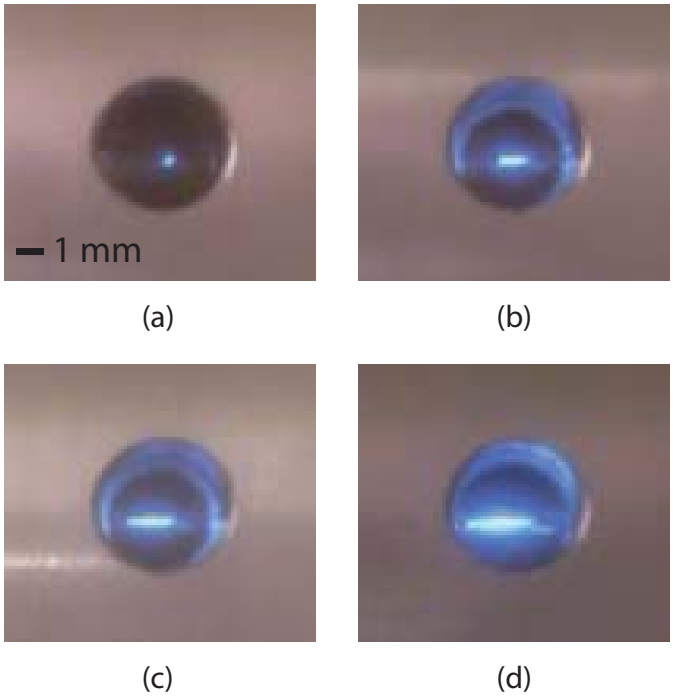

Fig. 4. Images of dielectric breakdown in the CS_2 cell at varying pulse energies. (a) 0.9 mJ, (b) 3.6 mJ, (c) 9.9 mJ, and (d) 17.7 mJ. The images are taken through a hole in the top of the CS_2 cell and the beam is propagating from left to right.

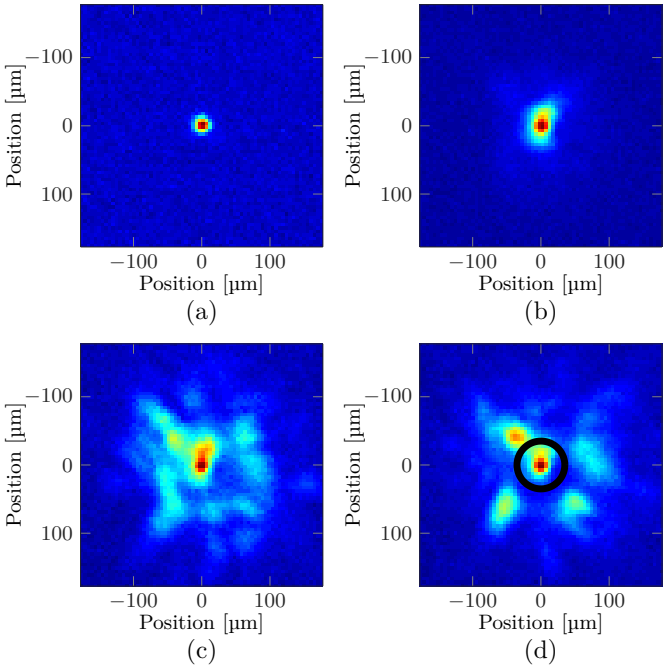

Fig. 5. Image of the beam at the focus position in the CS_2 cell. (a) low pulse energy, (b) 7 mJ, (c) 23 mJ, (d) 32 mJ. The black circle in (d) corresponds to how an aperture with diameter 1.4 mm in the position of AP_2 would block parts of the beam.

window, as expected from the moving-focus model. Estimating the threshold for self-focusing using the formula [26, 27]

$$P_{\mathrm{cr}} = 0.146\frac{\lambda^2}{n_0\gamma}, \tag{5}$$

gives $P_{\mathrm{cr}} = 128$ kW, corresponding to a pulse energy of 3.2 mJ for a SLM pulse with duration of 25 ns. The observed threshold for dielectric breakdown at 0.8 mJ is significantly lower than the estimated threshold for self-focusing. This indicates that dielectric breakdown happens independent of self-focusing, but could also be due to high-power spikes in the pulses, because the Ho:YLF pulses were MLM.

B.2. Imaging the beam at focus

The beam profile at the focus position in the CS_2 cell was imaged with a magnification $M = 20$ by placing a pyroelectric camera in the position of the aperture AP_2. Figure 5 shows the beam profile at different pulse energies. Laser beam breakup is clearly apparent in Fig. 5(c) and (d). The images in Fig. 5 represent single pulses, and the filament pattern varied significantly from pulse to pulse, even though the input energy was kept constant. As explained in Sec. B, we measured the encircled energy by using an aperture AP_2 with diameter 1.4 mm. In Fig. 5(d) it is indicated how such an aperture would block parts of the beam. We can estimate the peak fluence in the image as

$$F_{\mathrm{max}} \approx \frac{2E_{\mathrm{en}}}{\pi(M\omega_0)^2}, \tag{6}$$

where E_{en} is the encircled energy and ω_0 is the beam waist radius in the CS_2 cell. We measured a maximum encircled energy of 0.6 mJ. This gives $F_{\mathrm{max}} \approx 0.15M^{-2}$ kJ/cm^2. Here we have $M = 20$, giving $F_{\mathrm{max}} \approx 0.4$ J/cm^2. Equation (6) can be used to estimate the peak fluence for other focal lengths of the lens L_4. The minimum practical focal length of L_4 is about 10 mm, which gives $M = 0.2$ and $F_{\mathrm{max}} \approx 4$ kJ/cm^2. In this case further attenuation of the beam is needed, and a possible solution would be a tandem setup, where CS_2 is used in the first limiter stage [2].

No laser beam breakup was observed in an air-filled cell, proving that the filament pattern was indeed due to self-focusing, because air has a nonlinear coefficient which is a factor $\sim 10^5$ lower than CS_2 [19].

B.3. Measuring the encircled energy

Figure 6 shows measured transmission through the CS_2 cell and the limiting aperture as a function of pulse energy incident on the CS_2 cell, where we have corrected for losses in the uncoated cell windows. We observe from the measurements that transmission starts to decrease for an incident pulse energy of $\sim$0.8 mJ. As noted in Sec. B.1, the decrease in transmission was caused by dielectric breakdown, as in Fig. 4(a). We observed that there was an input energy range (0.6-0.9 mJ) where only some of the pulses led to dielectric breakdown. This may be due to the fact that the laser operates on multiple longitudinal modes, such that the peak power varied from pulse to pulse, even though the pulse energy was the same. Figure 6 shows that the transmission is approximately inversely proportional to the input pulse energy above the threshold for dielectric breakdown. This is equivalent to a constant transmitted pulse energy at high input energies. An analysis of the raw data showed that the transmitted energy through the limiting aperture never exceeded 0.6 mJ, even though the input energy was as high as 150 mJ. The constant transmitted pulse energies at high input energies is supported by Fig. 5, which shows that the energy of the central part of the beam is approximately constant when the

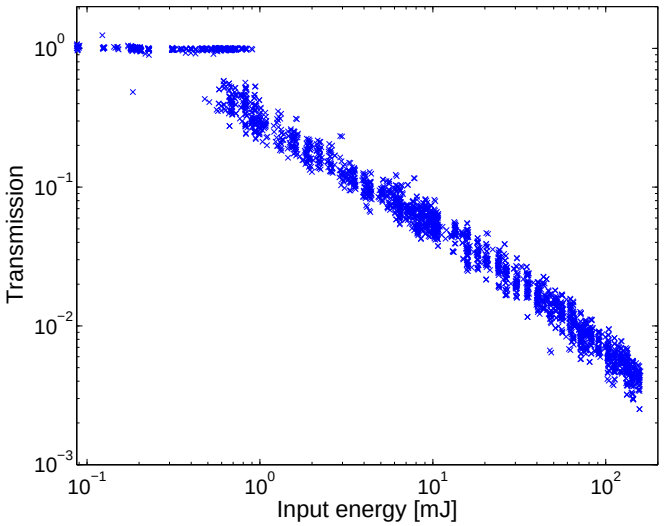

Fig. 6. Measured transmission through the limiting aperture AP_2 as a function of input energy on the CS_2 cell.

input energy increases.

Based on Figs. 4–6, we obtain the following picture of the optical limiting mechanisms: The start of the pulse, where the power is less than the limit for dielectric breakdown and self-focusing, will be transmitted linearly through the cell, with little attenuation. At some point in the pulse, the intensity will exceed the threshold for dielectric breakdown, which will generate a plasma that attenuates later parts of the pulse. At still later times, self-focusing will move the focus position towards the input window. At even later times, the beam will break up into several filaments. As shown in Fig. 5, the filaments will spread the pulse energy over a larger area. The total effect is that only the first part of the pulse is transmitted through the limiting aperture AP_2, regardless of input pulse energy.

5. CONCLUSION

The optical limiting properties of CS_2 at 2 μm wavelength have been studied. In addition, z-scan measurements were carried out to measure the nonlinear refractive index γ and the nonlinear absorption coefficient β of CS_2. The value of γ was found to be $(1.9 \pm 0.5) \cdot 10^{-18}$ m^2/W, i.e. $(7.2 \pm 1.9) \cdot 10^{-12}$ esu, for 25 ns pulses. The value of β was too low to be measured with this setup, but an upper limit is $2 \cdot 10^{-13}$ m/W. A larger value than this would lead to a detectable signal in the z-scan measurements with open aperture. In experiments where CS_2 was used as an optical limiter we found that beam filamentation and dielectric breakdown at the beam focus in the CS_2 cell were responsible for the limiting properties. Pulse energies up to 150 mJ were incident on the cell, while the encircled energy transmitted through a limiting aperture never exceeded 0.6 mJ. If further attenuation of the beam is needed, a tandem setup, consisting of two different limiting materials, where CS_2 is used in the first stage, could be considered.

APPENDIX A: AVERAGE NONLINEAR PHASE SHIFT FOR MULTIPLE LONGITUDINAL MODES

We will here derive an expression for the average nonlinear phase shift for the case of an arbitrary number of longitudinal modes and show that in the limit of an infinite number of longitudinal modes the average nonlinear phase shift is twice the phase shift compared to the case of a single longitudinal mode. Assuming instantaneous nonlinear response, the average nonlinear phase shift is given by [10]

$$\langle \Delta\Phi(t) \rangle = k\gamma L_{\text{eff}} \frac{\int_{-\infty}^{\infty} I^2(t)\mathrm{d}t}{\int_{-\infty}^{\infty} I(t)\mathrm{d}t}. \tag{7}$$

Assume an E-field on the form

$$E(t) = A(t)e^{j\omega_0 t}, \tag{8}$$

where

$$A(t) = \sum_{l=-n}^{l=n} a_l e^{jl\Delta\omega t}. \tag{9}$$

We have here assumed that there is a number $2n+1$ longitudinal modes with frequency spacing $\Delta\omega$. Assume further, for simplicity, that all frequency components l have identical magnitude but random phase, $a_l = E_0\alpha_l$, where $|\alpha_l| = 1$. Thus

$$A(t) = E_0 \sum_{l=-n}^{l=n} \alpha_l e^{jl\Delta\omega t}. \tag{10}$$

By insertion into Eq. (10), we observe that $A(t + 2\pi/\Delta\omega) = A(t)$. The average intensity thus becomes

$$\begin{aligned} \bar{I}(t) &= \frac{\Delta\omega}{2\pi}\int_0^{2\pi/\Delta\omega} |A(t)|^2 \mathrm{d}t \\ &= \frac{\Delta\omega}{2\pi}|E_0|^2 \sum_{l,l'} \alpha_l \alpha_{l'}^* \int_0^{2\pi/\Delta\omega} e^{j(l-l')\Delta\omega t}\mathrm{d}t. \end{aligned} \tag{11}$$

By carrying out the integration, we obtain

$$\bar{I}(t) = |E_0|^2 \sum_l |\alpha_l|^2 = (2n+1)|E_0|^2. \tag{12}$$

We then consider the average of the intensity squared,

$$\begin{aligned} \bar{I^2}(t) &= \tfrac{\Delta\omega}{2\pi}\int_0^{2\pi/\Delta\omega} |A(t)|^4 \mathrm{d}t \\ &= \tfrac{\Delta\omega}{2\pi}|E_0|^4 \textstyle\sum_{l,l',l'',l'''} \alpha_l \alpha_{l'}^* \alpha_{l''} \alpha_{l'''}^* \int_0^{2\pi/\Delta\omega} e^{j(l-l'+l''-l''')\Delta\omega t}\mathrm{d}t. \end{aligned} \tag{13}$$

By carrying out the integration, we obtain

$$\bar{I^2}(t) = |E_0|^4 \sum_{l,l',l'',l'''} \alpha_l \alpha_{l'}^* \alpha_{l''} \alpha_{l'''}^* \delta_{l+l'',l'+l'''}, \tag{14}$$

where $\delta_{i,j}$ is Kronecker's delta. Consider first the terms where $l = l'$. Then $l'' = l'''$ because of the Kronecker delta, and the sum is $(2n+1)^2$. Furthermore, for the case where $l = l'''$, we have $l' = l''$, due to the Kronecker delta, and the sum is also $(2n+1)^2$. We then obtain

$$\begin{aligned} \bar{I^2}(t) &= |E_0|^4 \\ &\cdot \left[2(2n+1)^2 - (2n+1) + \textstyle\sum_{l\neq l', l\neq l'''} \alpha_l \alpha_{l'}^* \alpha_{l''} \alpha_{l'''}^* \delta_{l+l'',l'+l'''}\right]. \end{aligned} \tag{15}$$

We have subtracted $(2n+1)$, because the terms where $l = l' = l'' = l'''$ are counted twice in the $2(2n+1)^2$ term. Because of the assumption of random phases, the mean value of the remaining sum in Eq. (15) will be zero. Thus, averaged over a large number of measurements, one can neglect the remaining sum in Eq. (15). We then obtain

$$\begin{aligned} \langle \Delta\Phi(t) \rangle_{\text{mlm}} &= k\gamma L_{\text{eff}} \frac{\left[2(2n+1)^2 - (2n+1)\right]|E_0|^4}{(2n+1)|E_0|^2} \\ &= \left(2 - \frac{1}{N}\right) k\gamma L_{\text{eff}} \bar{I}, \end{aligned} \tag{16}$$

where $N = 2n + 1$ is the number of longitudinal modes, and we have used the expression in Eq. (12) for $\bar{I}$. In the case of a monochromatic beam, with a single longitudinal mode ($N = 1$), we obtain

$$\langle \Delta\Phi(t) \rangle_{\mathrm{slm}} = k\gamma L_{\mathrm{eff}} \bar{I}. \tag{17}$$

Thus, the average nonlinear phase shift increases by a factor

$$\frac{\langle \Delta\Phi(t) \rangle_{\mathrm{mlm}}}{\langle \Delta\Phi(t) \rangle_{\mathrm{slm}}} = \left(2 - \frac{1}{N}\right) \tag{18}$$

for a multi-longitudinal-mode beam, compared to a single-longitudinal-mode beam, if they have the same average intensity $\bar{I}$. In the limit of an infinite number of longitudinal modes ($N \to \infty$), the factor becomes 2. This result is similar to the case of second-harmonic generation of a multiple longitudinal mode laser [13, 14].

REFERENCES

1. R. M. Wood, *Laser-induced damage of optical materials* (Institute of Physics, Bristol, UK, 2003).
2. F. E. Hernández, S. Yang, E. W. Van Stryland, and D. J. Hagan, "High-dynamic-range cascaded-focus optical limiter," Optics Letters **25**, 1180–1182 (2000).
3. M. J. Soileau, W. E. Williams, and E. W. Van Stryland, "Optical power limiter with picosecond response time," IEEE Journal of Quantum Electronics **QE-19**, 731–735 (1983).
4. L. W. Tutt and T. F. Boggess, "A review of optical limiting mechanisms and devices using organics, fullerenes, semiconductors and other materials," Prog. Quant. Electr. **17**, 299–338 (1993).
5. A. Couairon and A. Mysyrowicz, "Femtosecond filamentation in transparent media," Physics Reports **441**, 47–189 (2007).
6. P. P. Ho and R. R. Alfano, "Optical Kerr effect in liquids," Physical Review A **20**, 2170–2187 (1979).
7. Z.-B. Liu, Y.-L. Liu, B. Zhang, W.-Y. Zhou, J.-G. Tian, W.-P. Zang, and C.-P. Zhang, "Nonlinear absorption and optical limiting properties of carbon disulfide in a short-wavelength region," J. Opt. Soc. Am. B **24**, 1101–1104 (2007).
8. M. Mohebi, M. J. Soileau, and E. W. Van Stryland, "Resolution of discrepancies in measured values of n_2 of CS_2 at 10 μm," Optics Letters **13**, 649–650 (1988).
9. H. Fonnum, E. Lippert, and M. W. Haakestad, "550 mJ Q-switched cryogenic Ho:YLF oscillator pumped with a 100 W Tm:fiber laser." Optics Letters **38**, 1884–6 (2013).
10. M. Sheik-Bahae, A. A. Said, T. H. Wei, D. J. Hagan, and E. W. Van Stryland, "Sensitive measurement of optical nonlinearities using a single beam," IEEE Journal of Quantum Electronics **26**, 760–769 (1990).
11. R. A. Ganeev, A. I. Ryasnyansky, M. Baba, M. Suzuki, N. Ishizawa, M. Turu, S. Sakakibara, and H. Kuroda, "Nonlinear refraction in CS_2," Appl. Phys. B **78**, 433–438 (2004).
12. M. Reichert, H. Hu, M. R. Ferdinandus, M. Seidel, P. Zhao, T. R. Ensley, D. Peceli, J. M. Reed, D. A. Fishman, S. Webster, D. J. Hagan, and E. W. V. Stryland, "Temporal, spectral, and polarization dependence of the nonlinear optical response of carbon disulfide," Optica **1**, 436–445 (2014).
13. N. Bloembergen, *Nonlinear Optics* (W. A. Benjamin Inc., New York, 1965).
14. S. Helmfrid and G. Arvidsson, "Second-harmonic generation in quasi-phase-matching waveguides with a multimode pump," J. Opt. Soc. Am. B **8**, 2326–2330 (1991).
15. L. G. Holmen and M. W. Haakestad, "Optical limiting properties of carbon disulfide at 2.05 μm wavelength," Proc. SPIE **9731** (2016). Doi:10.1117/12.2206068.
16. E. K. Plyler and C. J. Humphreys, "Infrared absorption spectrum of carbon disulfide," Journal of Research of the National Bureau of Standards **39**, 59–65 (1947).
17. S. Kedenburg, M. Vieweg, T. Gissibl, and H. Giessen, "Linear refractive index and absorption measurements of nonlinear optical liquids in the visible and near-infrared spectral region," Opt. Mater. Express **2**, 1588–1611 (2012).
18. K. J. Witte, M. Galanti, and R. Volk, "n_2-measurements at 1.32 μm of some organic compounds usable as solvents in a saturable absorber for an atomic iodine laser," Optics Communications **34**, 278–282 (1980).
19. D. N. Nikogosyan, *Properties of optical and laser-related materials* (Wiley, West Sussex, England, 1997).
20. R. A. Ganeev, A. I. Ryasnyansky, N. Ishizawa, M. Baba, M. Suzuki, M. Turu, S. Sakakibara, and H. Kuroda, "Two- and three-photon absorption in CS_2," Optics Communications **231**, 431–436 (2004).
21. G. Seifert and H. Graener, "Mid-IR studies of third-order nonlinear optical susceptibilities with picosecond pulses," Optics Communications **115**, 216–224 (1995).
22. I. Golub, "Contribution of different nonlinear mechanisms in measurements of n_2 of CS_2 at 10 μm," Applied Optics **29**, 4428–30 (1990).
23. O. Uteza, B. Bussière, F. Canova, J. P. Chambaret, P. Delaporte, T. Itina, and M. Sentis, "Laser-induced damage threshold of sapphire in nanosecond, picosecond and femtosecond regimes," Applied Surface Science **254**, 799–803 (2007).
24. E. W. Van Stryland and M. Sheik-Bahae, "Z-scan measurements of optical nonlinearities," in "Characterization Techniques and Tabulations for Organic Nonlinear Materials," , M. G. Kuzyk and C. W. Dirk, eds. (Marcel Dekker, Inc., 1998), pp. 655–692.
25. N. Slavinskis, E. Murauskas, and A. S. Dement'ev, "Dependence of z-scan measurements on the spatiotemporal pulse parameters," Lithuanian Journal of Physics **51**, 127–135 (2011).
26. R. W. Boyd, *Nonlinear Optics* (Academic Press, San Diego, 2003).
27. J. H. Marburger, "Self-focusing: Theory," Prog. Quant. Electr. **4**, 35–110 (1975).